

# Tunable nonlinear spectra of anti-directional couplers

A. GOVINDARAJAN<sup>1,\*</sup>, BORIS A. MALOMED<sup>2</sup>, AND M. LAKSHMANAN<sup>1</sup>

<sup>1</sup>Centre for Nonlinear Dynamics, School of Physics, Bharathidasan University, Tiruchirappalli - 620 024, India

<sup>2</sup>Department of Physical Electronics, School of Electrical Engineering, Faculty of Engineering, and the Center for Light-Matter Interaction, Tel Aviv University, 69978 Tel Aviv, Israel

\*Corresponding author: govind.nld@gmail.com

Compiled September 17, 2021

We produce transmission and reflection spectra of the anti-directional coupler (ADC) composed of linearly-coupled positive- and negative-refractive-index arms, with intrinsic Kerr nonlinearity. Both reflection and transmission feature two highly amplified peaks at two distinct wavelengths in a certain range of values of the gain, making it possible to design a wavelength-selective mode-amplification system. We also predict that a blend of gain and loss in suitable proportions can robustly enhance reflection spectra which are detrimentally affected by the attenuation, in addition to causing red and blue shifts owing to the Kerr effect. In particular, ADC with equal gain and loss coefficients, is considered in necessary detail. © 2021 Optical Society of America

**OCIS codes:** (190.0190) Nonlinear optics; (160.3918) Metamaterials; (190.3270) Kerr effect; (060.1810) Buffers, couplers, routers, switches, and multiplexers; (300.6170) Spectra.

<http://dx.doi.org/10.1364/JB.XX.XXXXXX>

Metamaterials, alias left-handed media, are designed to exhibit unusual light-guiding characteristics, ranging from a negative refractive index (NRI) to magnetism at optical frequencies, owing to their controllable dielectric and magnetic properties [1–4]. While the concept of engineered NRI materials has drawn paramount interest [5], to utilize the extraordinary light-guiding capabilities of metamaterials in applications it is necessary to address remaining issues [6–9]. Among them, losses stand out as a major hindrance. Considerable efforts have been invested to compensate the losses originating from inherent attenuation in metallic elements of metamaterials, surface irregularities, magnetic resonances, and quantum effects [2, 10, 11].

One of the recently developed ramifications of studies of left-handed media is the design of anti-directional couplers (ADCs), composed of linearly coupled arms which are fabricated of positive-refractive-index (PRI) and NRI materials, see Fig. 1. Although the ADC resembles conventional gain-loss dimers, the contrast between its arms gives rise to light-guiding characteristics similar to those of distributed feedback structures, such as Bragg gratings, due to opposite signs of the Poynting vector ( $\vec{S}$  in Fig. 1) and phase velocities in the parallel-coupled NRI and PRI channels [5, 12–14]. Accordingly, ADC models exhibit both forward and backward propagation and optical bi-

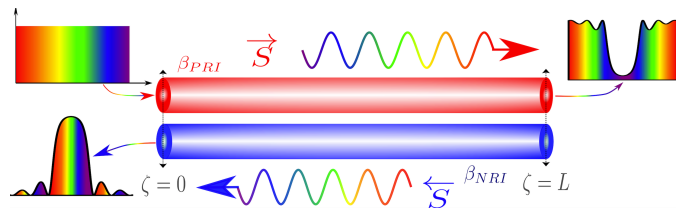


**Fig. 1.** A schematic of spectral dynamics in anti-directional couplers (ADCs) with gain and loss.

and multi-stabilities, in addition to the formation of nonstationary localized modes and discrete solitons in waveguide arrays [15]. However, the intrinsic dissipation of the NRI arm demands the use of large input intensities, which impairs possible applications to all-optical signal processing [12], filters [16], and amplifiers [17].

Recently, Walasik *et al.* have demonstrated that dissimilar linearly-coupled waveguides with complex refractive-index profiles, including gain and loss, may maintain meta- $\mathcal{PT}$ -symmetric nature of the coupler, supporting localized modes with real wave numbers [18], and thus extending the concept of stable solitons in  $\mathcal{PT}$ -symmetric nonlinear couplers [19–21]. Also, it has been shown that  $\mathcal{PT}$ -symmetric dimers can operate as efficient all-optical soliton switches with low input intensities [22]. Recent work [23] has laid a foundation of a new type of lasing systems exhibiting *resonant amplification* in ADCs. Motivated by those findings, we have demonstrated that the interplay of independently controlled amplification and attenuation enables novel bi- and multistable characteristics of ADCs [14]. These results suggest that ADCs may exhibit quasi- $\mathcal{PT}$ -symmetric-like operation, even in the absence of strictly symmetric and anti-symmetric arrangements of permittivity and gain/loss profiles. However, to the best of our knowledge no work has reported so far systematic investigation of nonlinear transmission and reflection spectra of ADCs. We here focus on this subject, with the intention to analyze the effects of the gain and loss strengths in the coupled channels on the nonlinear spectra, and propose feasible applications to all-optical signal-processing networks.

Coupled-mode equations for the light propagation in the nonlinear ADC, with balanced gain and loss in the PRI and NRI

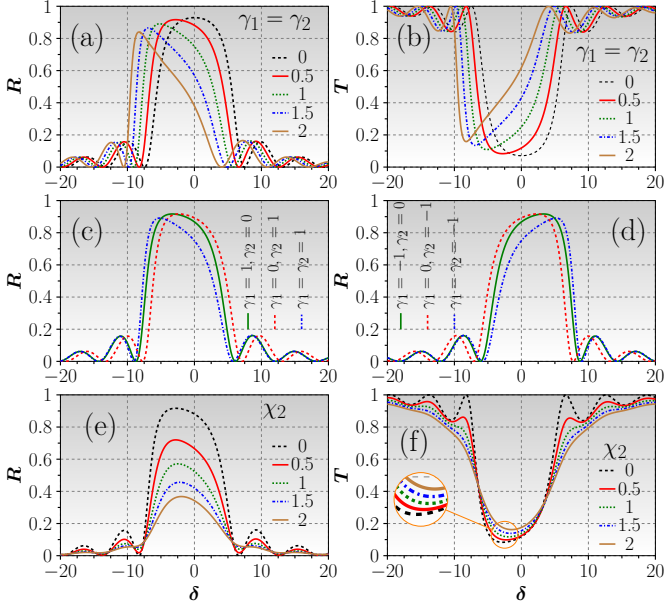


**Fig. 2.** Top panels show the nonlinear light dynamics, including the reflection and transmission, in the conservative symmetric ADC without gain and loss ( $\chi_1 = \chi_2 = 0$ ). In the middle panels, reflection spectra of the asymmetric ADC are shown with (c) self-focusing ( $\gamma_{1,2} \geq 0$ ) and (d) defocusing ( $\gamma_{1,2} \leq 0$ ) Kerr nonlinearities. The bottom panels exemplify the dynamics in the asymmetric nonlinear ADC with a lossy NRI core and the conservative PRI one ( $\chi_1 = 0$ ), with Kerr coefficients  $\gamma_1 = \gamma_2 = 0.5$ .

channels, are written as [12, 14]

$$+i \frac{dF(\zeta)}{d\zeta} + \gamma_1 |F(\zeta)|^2 F(\zeta) + \kappa B(\zeta) e^{-i\delta\zeta} = i\chi_1 F(\zeta), \quad (1)$$

$$-i \frac{dB(\zeta)}{d\zeta} + \gamma_2 |B(\zeta)|^2 B(\zeta) + \kappa F(\zeta) e^{i\delta\zeta} = -i\chi_2 B(\zeta), \quad (2)$$

where  $\zeta$  is the longitudinal coordinate,  $F(\zeta)$  and  $B(\zeta)$  are complex amplitudes of forward- and backward-traveling waves in the PRI and NRI channels,  $\gamma_{1,2}$  are Kerr coefficients in the channels, and detuning  $\delta = \beta_{\text{PRI}} - \beta_{\text{NRI}} \equiv 2\pi (n_F - n_B) / \lambda$  is the difference between modal wavenumbers in the channels, which is determined by modal indices,  $n_{F,B}$ , and vacuum wavelength,  $\lambda$ . As concerns the inter-core linear coupling, although its effective coefficients may be different in the two channels, we adopt equal coefficients,  $\kappa$ , to focus on the impact of intra-channel gain ( $\chi_1$ ) and loss ( $\chi_2$ ).

First, we produce nonlinear spectra as a function of detuning  $\delta$  (for linear spectra, one can refer to Ref. [23]), with a fixed intensity of the incident signal,  $|F(\zeta = 0)|^2$ . To this end, we integrate the coupled-mode equations (1) and (2) by using the Dormand-Prince method [24] with appropriate boundary conditions, keeping scaled values of the system's parameters, including the ADC's length,  $L$ , as  $\gamma_{1,2} = L = 1$  and  $\kappa = 2$ , unless stated otherwise. Then, we define the transmissivity as  $T = |F(\zeta = L) / F(\zeta = 0)|^2$ , where  $|F(\zeta = L)|^2$  is the output intensity in the PRI channel. As shown in Fig. 2(a), in the ideal (conservative) coupler ( $\chi_1 = \chi_2 = 0$ ), which does not include loss and gain, the Kerr nonlinearity, with  $\gamma_1 = \gamma_2 = \gamma$ , shifts the spectral resonance of the reflectivity,  $R \equiv |B(\zeta = 0) / F(\zeta = 0)|^2$ , from its position at  $\delta = 0$  (pertaining to the photonic bandgap,

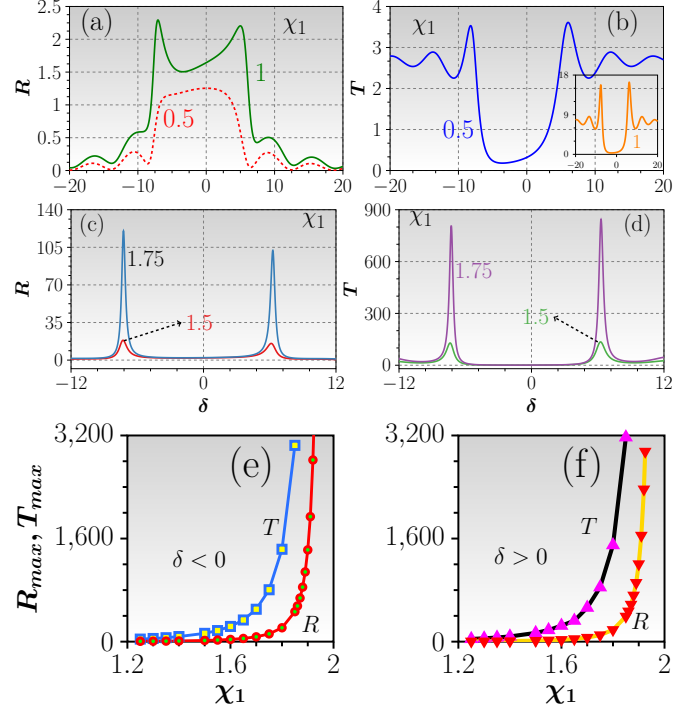


**Fig. 3.** Gain-induced ( $\chi_1$ ) mode-selective amplification in the reflection and transmission spectra of nonlinear ADC with  $\gamma_1 = \gamma_2 = 1$ , with the gain ( $\chi_1 = 1$ ) applied to the PRI channel, while the NRI one remains neutral ( $\chi_2 = 0$ ).

alias *stopband*, where the spectrum features relatively high (low) reflection (transmission). Further enhancement of the nonlinearity results in a farther *red shift* of the spectrum towards longer wavelengths, with a narrow peak appearing at the top of the reflectivity spectrum, as seen in Figs. 2(a). Similar peculiarities are observed in the transmission spectra in the PRI channel, see Fig. 2(b). These panels comply with the unitary condition,  $T + R = 1$ , in the conservative ADC. Unlike the Bragg-grating structures, the light-transfer characteristics of the ADC is underlain by the transfer of power between the two cores. Therefore, it is possible to control the transmissivity and reflectivity by independently adjusting the nonlinearity in the two cores. Accordingly, in Figs. 2(c,d) we display the spectra for the asymmetric conservative system, in which either one of the cores (PRI or NRI channel) is linear and the other one is nonlinear. The plots in Figs. 2(c,d) for the ADC with the linear NRI or PRI channel (see dashed red and solid blue lines, respectively) feature a spectral shift towards positive or negative detuning.

The ADC with self-defocusing Kerr nonlinearities ( $\gamma_{1,2} < 0$ ) exhibits opposite trends, *viz.*, a *blue shift* of the spectra towards shorter wavelengths. The respective transmission spectra reveal features similar to those exhibited in Figs. 2(c,d), and are not displayed here. All these ramifications clearly indicate that one can easily tune the ADC spectra with the help of the Kerr nonlinearities in the NRI and PRI channels. Physically, the origin of the tunability (shifting) of the spectra can be understood as follows: the change in the focusing Kerr nonlinear coefficient results in an increase of the effective refractive index, which eventually shifts the photonic bandgap, thus causing the red shift of the spectra. Similarly, the change of the defocusing nonlinear coefficient causes a reduction of the refractive index, leading to the blue shift. As concerns potential applications of such reflection

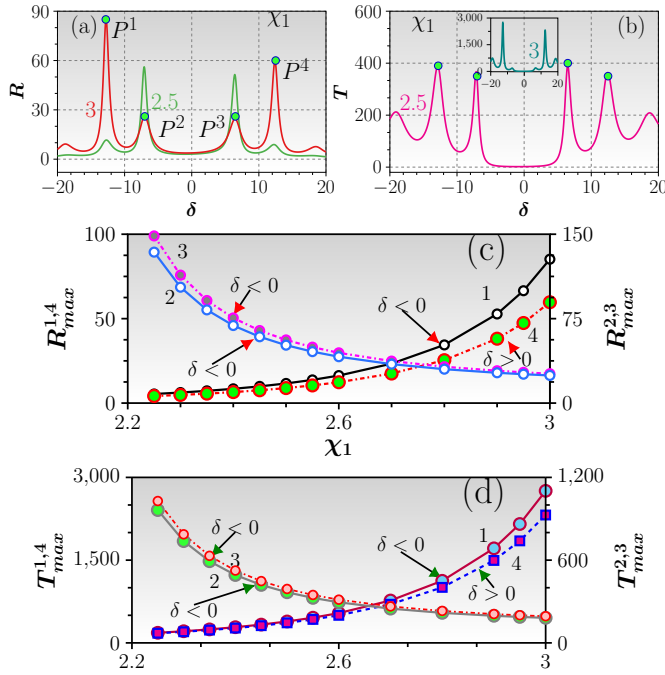


**Fig. 4.** (a,b) Dependence of strong secondary spectral resonances of the reflectivity and transmissivity on the variation of gain in the PRI channel. The corresponding maximum reflectivity and transmissivity for different numbers of spectral peaks (denoted by  $P^{1,2,3,4}$ ) are shown in (c,d). The system's parameters are the same as in Fig. 3.

and transmission spectra due to the Kerr nonlinearity, the ability to shift both of them with respect to the input wavelengths is a vital asset for the use in all-optical signal processing, including the design of band-selection filters, mode converters, and wavelength demultiplexers [25].

To elucidate the detrimental role of the intrinsic loss,  $\chi_2$ , in the NRI channel, without adding gain to the PRI one, Fig. 2(e) demonstrates that the corresponding reflection band in the NRI channel suffers suppression of both its magnitude and width with the increase of  $\chi_2$ . On the other hand, the transmission spectra show only marginal changes in Fig. 2(f), under the variation of  $\chi_2$ . A noteworthy effect is observed near the edges of the stopband (where zero transmission takes place), in the form of red shift, while a blue shift is found outside of the stopband. Thus, a conclusion is that the loss in the NRI channel of ADC leads to severe suppression of the reflection spectra, while the characteristic transmission spectra are not strongly affected.

Figure 3 displays the calculated reflection and transmission spectra of the ADC with gain applied in the PRI core, while keeping zero loss in the NRI one. With gain  $\chi_1 = 0.5$ , the reflectivity naturally features a maximum in the stopband in Fig. 3(a), while decaying to zero outside of it. The increase of the gain to  $\chi_1 = 1$  leads to splitting of the reflectivity maximum in two peaks located near the edges of the stopband. The transmission spectrum corresponding to Fig. 3(a) is displayed in Fig. 3(b), which exhibits growing peaks on both sides of the stopband. It further increases rapidly with the increment of  $\chi_1$ , see the inset in Fig. 3(b). In both the reflection and transmission spectra as seen in Figs. 3(c,d), the peaks feature extremely strong amplification at  $\chi_1 = 1.5$  and  $1.75$ , which is further observed in Figs. 3(e,f), where the maxima in  $R$  and  $T$  for different values of  $\chi_1$  are

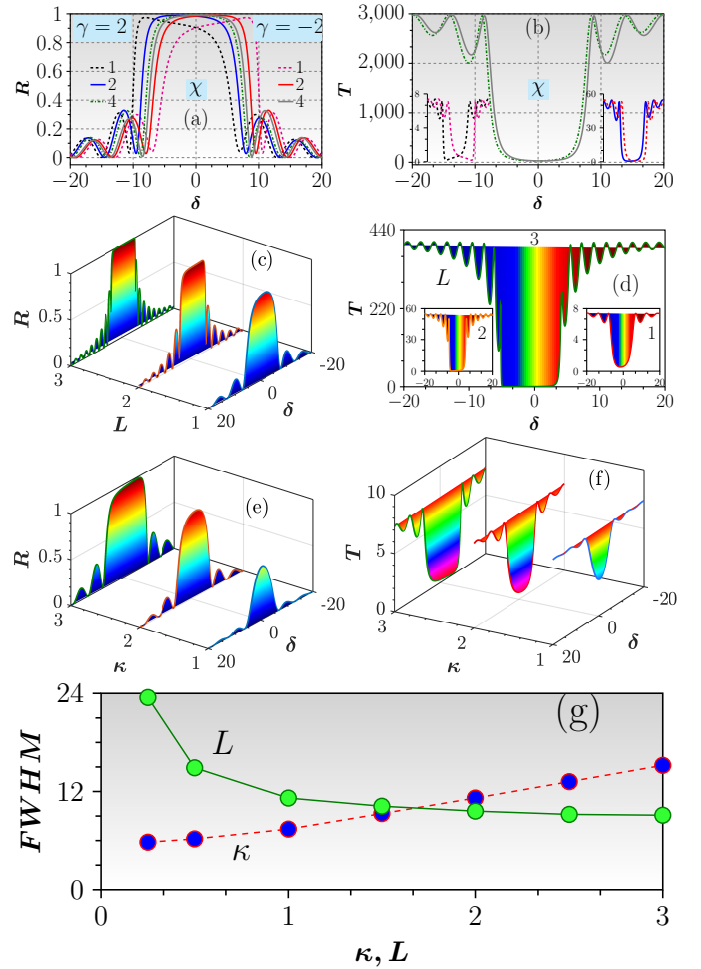


**Fig. 5.** (a,b) Nonlinear reflection and transmission spectra as a function of mismatch  $\delta$  for the  $\mathcal{PT}$ -symmetric ADC, with equal gain and loss in the PRI and NRI cores ( $\chi_1 = \chi_2 \equiv \chi = 1$ ). Panels (c,d) and (e,f) show, respectively, the impact of the coupler's length,  $L$ , and the inter-core linear coupling,  $\kappa$ . The bottom panels display the bandwidth (FWHM) of the reflection spectra versus  $\kappa$  and  $L$ .

plotted for both  $\delta > 0$  and  $\delta < 0$ .

When the gain strength in the PRI channel increases beyond  $\chi_1 \approx 2$ , remarkable mode-selective amplification occurs at four distinct wavelengths, two shorter and two longer ones, as seen in Figs. 4(a,b). In particular, at  $\chi_1 = 2.5$ , the two peaks near the edges of the stopband feature more amplification than those found outside of the stopband. On the contrary, when  $\chi_1 = 3$ , the pair of peaks outside the stopband show giant amplification, while the two others, close to the edges of the stopband, are suppressed, in comparison with their counterparts at  $\chi_1 = 2.5$ . This trend is confirmed by the dependence of the peak reflectivity on continuous variation of the gain in the PRI channel, as shown in Fig. 4(c). A similar amplification pattern is exhibited by the corresponding transmission spectra in Figs. 4(b) and 4(d), with a difference that the magnitude of the amplification is much higher in comparison with the reflectivity.

The studies of  $\mathcal{PT}$ -symmetric systems have drawn a great deal of interest in couplers with equal magnitudes of gain and loss in two parallel-coupled cores [19]-[21], [26, 27], [14]. Results for this case are collected in Fig. 5. First, it is relevant

to stress the effects of equal gain-loss coefficients on the ADC spectra. As the value of the gain-loss increases, the spectrum shifts towards shorter or longer wavelengths if the nonlinearity is, respectively, self-focusing or defocusing in both the amplified gain and lossy channels, as seen in Fig. 5(a). In Fig. 5(b), the transmission spectra exhibit spectral resonances with huge amplification, without attaining any lasing behavior, even if the gain is very large, in comparison to the spectra in the absence of gain and loss. Further, in Fig. 5(a) it is seen that the increase of the self-focusing coefficient (in particular, to values  $\gamma_1 = \gamma_2 = 2$ ) in ADC with equal gain and loss gives rise to a stronger red shift in the nonlinear spectra. On the other hand, stronger self-defocusing nonlinearity drives the blue shift [see red solid and dashed lines in Figs. 5(a,b)]. In the system including both focusing and defocusing nonlinearities, the stopband remains flat, completely reflecting the incident light ( $R = 1$ ). This implies keeping ideal spectra, with the photonic bandgap staying in its original position, the same as in the linear system (which is not shown here). Even for the transmission spectra in the PRI channel, conclusions suggested by Fig. 5(a) remain true, as can be seen in Fig. 5(b). Note that here too, a distinctive feature of the nonlinear ADC is huge amplification in the transmission spectra, even in the presence of loss. Thus, the remarkable ability to control the flat broad stopband and the magnitude of the transmissivity by adjusting the values of the gain and loss coefficients and wavelength of the input signal makes the ADC an appropriate element for all-optical signal-processing and demultiplexing applications.

Finally, Fig. 5(c) shows that the ADC length plays an essential role in broadening or narrowing the spectral range, as well as in the enhancement of reflectivity. In particular, when  $L = 1$  and  $\kappa = 2$ , the spectral range is broad, but the peak value of the reflectivity is low. However, when the length increases to  $L = 2$ , the reflectivity in the stopband increases, while the spectrum shrinks. At  $L = 3$ , the reflectivity is nearly flat for wavelengths near  $\delta = 0$ , and its magnitude is close to 1. The respective transmission spectra exhibit similar peculiarities, but with transmissivity much higher than the reflectivity at the same parameters, see Fig. 5(d). Conversely, the region of the nearly flat spectrum in the stopband can be expanded and made still flatter (and closer to 1, as in the case of reflectivity) by increasing the strength of the inter-core coupling,  $\kappa$ , as seen in Fig. 5(e). Once again, the transmission spectra shown in Fig. 5(f) demonstrate a similar behavior, but with values of the transmissivity much larger than the corresponding reflectivity (by a factor of  $\simeq 8$ ). In both cases, it is worthy to note that the bandwidth of spectra decreases (increases) when the length (inter-core coupling parameter) is varied, as seen in Fig. 5(g).

In conclusion, we have shown that ADCs (anti-directional couplers) with the Kerr nonlinearity in their cores exhibit novel transmission and reflection spectra, which may be relevant to fundamental studies and potential applications. The gain applied to one of the two cores (the PRI channel) maintains the effect of the wavelength-selective amplification, while equal gain and loss acting in the two cores effectively restore both the reflection and transmission spectra, which are suppressed by the dominating loss. The former setting also gives rise to transmission and reflection spectra with a broad flat stopband, along with inducing red and blue shifts. These properties suggest that ADC may serve as an essential component in integrated light-wave data-processing systems. As an extension of the analysis, it may be relevant to consider a composite waveguide, built of periodically alternating ADC segments with switched NRI/PRI

structure. Previously, a similar setting composed of segments with periodically switching gain and loss segments was demonstrated to provide strong stabilization of  $\mathcal{PT}$ -symmetric solitons [28].

**Funding:** Science and Engineering Research Board (SERB) of India, PDF/2016/002933 and SB/DF/04/2017). Israel Science Foundation, grant No. 1286/17.

**Disclosures.** The authors declare no conflicts of interest.

## REFERENCES

1. V. M. Shalaev, W. Cai, U. K. Chettiar, H.-K. Yuan, A. K. Sarychev, V. P. Drachev, and A. V. Kildishev, *Opt. Lett.* **30**, 3356 (2005).
2. G. Dolling, C. Enkrich, M. Wegener, C. M. Soukoulis, and S. Linden, *Opt. Lett.* **31**, 1800 (2006).
3. J. Zeng, X. Wang, J. Sun, A. Pandey, A. N. Cartwright, and N. M. Litchinitser, *Sci. Rep.* **3**, 2826 (2013).
4. G. Dolling, M. Wegener, C. M. Soukoulis, and S. Linden, *Opt. Lett.* **32**, 53 (2007).
5. N. M. Litchinitser, *Science* **337**, 1054 (2012).
6. N. M. Litchinitser and V. M. Shalaev, *J. Opt. Soc. Am. B* **26**, B161 (2009).
7. S. A. Ramakrishna, *Rep. Prog. Phys.* **68**, 449 (2005).
8. M. Lapine, I. V. Shadrivov, and Y. S. Kivshar, *Rev. Mod. Phys.* **86**, 1093 (2014).
9. M. R. Hashemi, S. Cakmakyapan and M. Jarrahi, *Rep. Prog. Phys.* **80**, 094501 (2017).
10. A. K. Popov and V. M. Shalaev, *Opt. Lett.* **31**, 2169 (2006).
11. A. K. Popov, S. A. Myslivets, T. F. George, and V. M. Shalaev, *Opt. Lett.* **32**, 3044 (2007).
12. N. M. Litchinitser, I. R. Gabitov, and A. I. Maimistov, *Phys. Rev. Lett.* **99**, 113902 (2007).
13. G. Venugopal, Z. Kudyshev, and N. M. Litchinitser, *IEEE J. Sel. Top. Quantum Electron.* **18**, 753 (2011).
14. A. Govindarajan, B. A. Malomed, and M. Lakshmanan, *Opt. Lett.* **44**, 4650 (2019).
15. D. A. Zezyulin, V. V. Konotop, and F. K. Abdullaev, *Opt. Lett.* **37**, 3930 (2012).
16. P. Chu, G. Peng, B. Malomed, H. Hatami-Hanza, and I. Skinner, *Opt. Lett.* **20**, 1092 (1995).
17. B. A. Malomed, G. Peng, and P. Chu, *Opt. Lett.* **21**, 330 (1996).
18. W. Walasik, C. Ma, and N. M. Litchinitser, *New Journal of Physics* **19**, 075002 (2017).
19. R. Driben and B. A. Malomed, *Opt. Lett.* **36**, 4323 (2011).
20. F. K. Abdullaev, V. Konotop, M. Ögren, and M. P. Sørensen, *Opt. Lett.* **36**, 4566 (2011).
21. N. Alexeeva, I. Barashenkov, A. A. Sukhorukov, and Y. S. Kivshar, *Phys. Rev. A* **85**, 063837 (2012).
22. A. Govindarajan, A. K. Sarma, and M. Lakshmanan, *Opt. Lett.* **44**, 663 (2019).
23. B. A. Tennant, R. Ara, A. Atwiri, G. P. Agrawal, N. M. Litchinitser, and D. N. Maywar, *Opt. Lett.* **44**, 4586 (2019).
24. J. Dormand and P. Prince, *Celestial Mechanics* **18**, 223 (1978).
25. G. Agrawal and D. Maywar, Semiconductor optical amplifiers with bragg gratings, in *Nonlinear Photonic Crystals*, (Springer, 2003), pp. 285–300.
26. V. V. Konotop, J. Yang, and D. A. Zezyulin, *Rev. of Mod. Phys.* **88**, 035002 (2016).
27. S. V. Suchkov, A. A. Sukhorukov, J. Huang, S. V. Dmitriev, C. Lee, and Y. S. Kivshar, *Laser & Photonics Reviews* **10**, 177 (2016).
28. R. Driben and B. Malomed, *EPL (Europhysics Letters)* **96**, 51001 (2011).